7 March 1996

PHYSICS LETTERS B

ELSEVIER

Physics Letters B 370 (1996) 239–248

J/ψ production in $p\bar{p}$ collisions at $\sqrt{s} = 1.8$ TeV

DØ Collaboration

S. Abachi[n], B. Abbott[ab], M. Abolins[y], B.S. Acharya[ar], I. Adam[ℓ], D.L. Adams[ak], M. Adams[q], S. Ahn[n], H. Aihara[v], J. Alitti[an], G. Álvarez[r], G.A. Alves[j], E. Amidi[ac], N. Amos[x], E.W. Anderson[s], S.H. Aronson[d], R. Astur[ap], R.E. Avery[ae], A. Baden[w], V. Balamurali[af], J. Balderston[p], B. Baldin[n], J. Bantly[e], J.F. Bartlett[n], K. Bazizi[am], J. Bendich[v], S.B. Beri[ah], I. Bertram[ak], V.A. Bezzubov[ai], P.C. Bhat[n], V. Bhatnagar[ah], M. Bhattacharjee[m], A. Bischoff[i], N. Biswas[af], G. Blazey[n], S. Blessing[o], P. Bloom[g], A. Boehnlein[n], N.I. Bojko[ai], F. Borcherding[n], J. Borders[am], C. Boswell[i], A. Brandt[n], R. Brock[y], A. Bross[n], D. Buchholz[ae], V.S. Burtovoi[ai], J.M. Butler[c], W. Carvalho[j], D. Casey[am], H. Castilla-Valdez[k], D. Chakraborty[ap], S.-M. Chang[ac], S.V. Chekulaev[ai], L.-P. Chen[v], W. Chen[ap], S. Chopra[x], B.C. Choudhary[i], J.H. Christenson[n], M. Chung[q], D. Claes[ap], A.R. Clark[v], W.G. Cobau[w], J. Cochran[i], W.E. Cooper[n], C. Cretsinger[am], D. Cullen-Vidal[e], M.A.C. Cummings[p], D. Cutts[e], O.I. Dahl[v], K. De[as], M. Demarteau[n], R. Demina[ac], K. Denisenko[n], N. Denisenko[n], D. Denisov[n], S.P. Denisov[ai], H.T. Diehl[n], M. Diesburg[n], G. Di Loreto[y], R. Dixon[n], P. Draper[as], J. Drinkard[h], Y. Ducros[an], S.R. Dugad[ar], S. Durston-Johnson[am], D. Edmunds[y], J. Ellison[i], V.D. Elvira[f], R. Engelmann[ap], S. Eno[w], G. Eppley[ak], P. Ermolov[z], O.V. Eroshin[ai], V.N. Evdokimov[ai], S. Fahey[y], T. Fahland[e], M. Fatyga[d], M.K. Fatyga[am], J. Featherly[d], S. Feher[ap], D. Fein[b], T. Ferbel[am], G. Finocchiaro[ap], H.E. Fisk[n], Y. Fisyak[g], E. Flattum[y], G.E. Forden[b], M. Fortner[ad], K.C. Frame[y], P. Franzini[ℓ], S. Fuess[n], E. Gallas[as], A.N. Galyaev[ai], T.L. Geld[y], R.J. Genik II[y], K. Genser[n], C.E. Gerber[f], B. Gibbard[d], V. Glebov[am], S. Glenn[g], J.F. Glicenstein[an], B. Gobbi[ae], M. Goforth[o], A. Goldschmidt[v], B. Gómez[a], P.I. Goncharov[ai], J.L. González Solís[k], H. Gordon[d], L.T. Goss[at], N. Graf[d], P.D. Grannis[ap], D.R. Green[n], J. Green[ad], H. Greenlee[n], G. Griffin[h], N. Grossman[n], P. Grudberg[v], S. Grünendahl[am], W.X. Gu[n,l], G. Guglielmo[ag], J.A. Guida[b], J.M. Guida[e], W. Guryn[d], S.N. Gurzhiev[ai], P. Gutierrez[ag], Y.E. Gutnikov[ai], N.J. Hadley[w], H. Haggerty[n], S. Hagopian[o], V. Hagopian[o], K.S. Hahn[am], R.E. Hall[h], S. Hansen[n], R. Hatcher[y], J.M. Hauptman[s], D. Hedin[ad], A.P. Heinson[i], U. Heintz[n], R. Hernández-Montoya[k], T. Heuring[o], R. Hirosky[o], J.D. Hobbs[n], B. Hoeneisen[a,2], J.S. Hoftun[e], F. Hsieh[x], Tao Hu[n,l], Ting Hu[ap], Tong Hu[r], T. Huehn[i], S. Igarashi[n], A.S. Ito[n], E. James[b], J. Jaques[af], S.A. Jerger[y], J.Z.-Y. Jiang[ap], T. Joffe-Minor[ae], H. Johari[ac], K. Johns[b], M. Johnson[n], H. Johnstad[aq], A. Jonckheere[n], M. Jones[p], H. Jöstlein[n], S.Y. Jun[ae], C.K. Jung[ap], S. Kahn[d], G. Kalbfleisch[ag], J.S. Kang[t], R. Kehoe[af], M.L. Kelly[af], L. Kerth[v],

Elsevier Science B.V.
SSDI 0370-2693(96)00067-6

C.L. Kim[t], S.K. Kim[ao], A. Klatchko[o], B. Klima[n], B.I. Klochkov[ai], C. Klopfenstein[g], V.I. Klyukhin[ai], V.I. Kochetkov[ai], J.M. Kohli[ah], D. Koltick[aj], A.V. Kostritskiy[ai], J. Kotcher[d], J. Kourlas[ab], A.V. Kozelov[ai], E.A. Kozlovski[ai], M.R. Krishnaswamy[ar], S. Krzywdzinski[n], S. Kunori[w], S. Lami[ap], G. Landsberg[n], J-F. Lebrat[an], A. Leflat[z], H. Li[ap], J. Li[as], Y.K. Li[ae], Q.Z. Li-Demarteau[n], J.G.R. Lima[aℓ], D. Lincoln[x], S.L. Linn[o], J. Linnemann[y], R. Lipton[n], Y.C. Liu[ae], F. Lobkowicz[am], S.C. Loken[v], S. Lökös[ap], L. Lueking[n], A.L. Lyon[w], A.K.A. Maciel[j], R.J. Madaras[v], R. Madden[o], S. Mani[g], H.S. Mao[n,l], S. Margulies[q], R. Markeloff[ad], L. Markosky[b], T. Marshall[r], M.I. Martin[n], M. Marx[ap], B. May[ae], A.A. Mayorov[ai], R. McCarthy[ap], T. McKibben[q], J. McKinley[y], T. McMahon[ag], H.L. Melanson[n], J.R.T. de Mello Neto[aℓ], K.W. Merritt[n], H. Miettinen[ak], A. Mincer[ab], J.M. de Miranda[j], C.S. Mishra[n], M. Mohammadi-Baarmand[ap], N. Mokhov[n], N.K. Mondal[ar], H.E. Montgomery[n], P. Mooney[a], H. da Motta[j], M. Mudan[ab], C. Murphy[q], C.T. Murphy[n], F. Nang[e], M. Narain[n], V.S. Narasimham[ar], A. Narayanan[b], H.A. Neal[x], J.P. Negret[a], E. Neis[x], P. Nemethy[ab], D. Nešić[e], M. Nicola[j], D. Norman[at], L. Oesch[x], V. Oguri[aℓ], E. Oltman[v], N. Oshima[n], D. Owen[y], P. Padley[ak], M. Pang[s], A. Para[n], C.H. Park[n], Y.M. Park[u], R. Partridge[e], N. Parua[ar], M. Paterno[am], J. Perkins[as], A. Peryshkin[n], M. Peters[p], H. Piekarz[o], Y. Pischalnikov[aj], V.M. Podstavkov[ai], B.G. Pope[y], H.B. Prosper[o], S. Protopopescu[d], D. Pušeljić[v], J. Qian[x], P.Z. Quintas[n], R. Raja[n], S. Rajagopalan[ap], O. Ramirez[q], M.V.S. Rao[ar], P.A. Rapidis[n], L. Rasmussen[ap], A.L. Read[n], S. Reucroft[ac], M. Rijssenbeek[ap], T. Rockwell[y], N.A. Roe[v], P. Rubinov[ae], R. Ruchti[af], J. Rutherfoord[b], A. Santoro[j], L. Sawyer[as], R.D. Schamberger[ap], H. Schellman[ae], J. Sculli[ab], E. Shabalina[z], C. Shaffer[o], H.C. Shankar[ar], Y.Y. Shao[n,l], R.K. Shivpuri[m], M. Shupe[b], J.B. Singh[ah], V. Sirotenko[ad], W. Smart[n], A. Smith[b], R.P. Smith[n], R. Snihur[ae], G.R. Snow[aa], S. Snyder[d], J. Solomon[q], P.M. Sood[ah], M. Sosebee[as], M. Souza[j], A.L. Spadafora[v], R.W. Stephens[as], M.L. Stevenson[v], D. Stewart[x], D.A. Stoianova[ai], D. Stoker[h], K. Streets[ab], M. Strovink[v], A. Sznajder[j], A. Taketani[n], P. Tamburello[w], J. Tarazi[h], M. Tartaglia[n], T.L. Taylor[ae], J. Thompson[w], T.G. Trippe[v], P.M. Tuts[ℓ], N. Varelas[y], E.W. Varnes[v], P.R.G. Virador[v], D. Vititoe[b], A.A. Volkov[ai], A.P. Vorobiev[ai], H.D. Wahl[o], G. Wang[o], J. Warchol[af], G. Watts[e], M. Wayne[af], H. Weerts[y], F. Wen[o], A. White[as], J.T. White[at], J.A. Wightman[s], J. Wilcox[ac], S. Willis[ad], S.J. Wimpenny[i], J.V.D. Wirjawan[at], J. Womersley[n], E. Won[am], D.R. Wood[ac], H. Xu[e], R. Yamada[n], P. Yamin[d], C. Yanagisawa[ap], J. Yang[ab], T. Yasuda[ac], C. Yoshikawa[p], S. Youssef[o], J. Yu[am], Y. Yu[ao], D.H. Zhang[n,l], Q. Zhu[ab], Z.H. Zhu[am], D. Zieminska[r], A. Zieminski[r], E.G. Zverev[z], A. Zylberstejn[an]

[a] *Universidad de los Andes, Bogotá, Colombia*
[b] *University of Arizona, Tucson, AZ 85721, USA*
[c] *Boston University, Boston, MA 02215, USA*
[d] *Brookhaven National Laboratory, Upton, NY 11973, USA*
[e] *Brown University, Providence, RI 02912, USA*
[f] *Universidad de Buenos Aires, Buenos Aires, Argentina*
[g] *University of California, Davis, CA 95616, USA*
[h] *University of California, Irvine, CA 92717, USA*
[i] *University of California, Riverside, CA 92521, USA*

[j] LAFEX, Centro Brasileiro de Pesquisas Físicas, Rio de Janeiro, Brazil
[k] CINVESTAV, Mexico City, Mexico
[l] Columbia University, New York, NY 10027, USA
[m] Delhi University, Delhi, India 110007
[n] Fermi National Accelerator Laboratory, Batavia, IL 60510, USA
[o] Florida State University, Tallahassee, FL 32306, USA
[p] University of Hawaii, Honolulu, HI 96822, USA
[q] University of Illinois at Chicago, Chicago, IL 60607, USA
[r] Indiana University, Bloomington, IN 47405, USA
[s] Iowa State University, Ames, IA 50011, USA
[t] Korea University, Seoul, South Korea
[u] Kyungsung University, Pusan, South Korea
[v] Lawrence Berkeley National Laboratory and University of California, Berkeley, CA 94720, USA
[w] University of Maryland, College Park, MD 20742, USA
[x] University of Michigan, Ann Arbor, MI 48109, USA
[y] Michigan State University, East Lansing, MI 48824, USA
[z] Moscow State University, Moscow, Russia
[aa] University of Nebraska, Lincoln, NE 68588, USA
[ab] New York University, New York, NY 10003, USA
[ac] Northeastern University, Boston, MA 02115, USA
[ad] Northern Illinois University, DeKalb, IL 60115, USA
[ae] Northwestern University, Evanston, IL 60208, USA
[af] University of Notre Dame, Notre Dame, IN 46556, USA
[ag] University of Oklahoma, Norman, OK 73019, USA
[ah] University of Panjab, Chandigarh 16-00-14, India
[ai] Institute for High Energy Physics, 142-284 Protvino, Russia
[aj] Purdue University, West Lafayette, IN 47907, USA
[ak] Rice University, Houston, TX 77251, USA
[al] Universidade Estadual do Rio de Janeiro, Brazil
[am] University of Rochester, Rochester, NY 14627, USA
[an] CEA, DAPNIA/Service de Physique des Particules, CE-SACLAY, France
[ao] Seoul National University, Seoul, South Korea
[ap] State University of New York, Stony Brook, NY 11794, USA
[aq] SSC Laboratory, Dallas, TX 75237, USA
[ar] Tata Institute of Fundamental Research, Colaba, Bombay 400005, India
[as] University of Texas, Arlington, TX 76019, USA
[at] Texas A&M University, College Station, TX 77843, USA

Received 11 January 1996
Editor: L. Montanet

Abstract

We have studied J/ψ production in $p\bar{p}$ collisions at $\sqrt{s} = 1.8$ TeV with the DØ detector at Fermilab using $\mu^+\mu^-$ data. We have measured the inclusive J/ψ production cross section as a function of J/ψ transverse momentum, p_T. For the kinematic range $p_T > 8$ GeV/c and $|\eta| < 0.6$ we obtain $\sigma(p\bar{p} \to J/\psi + X) \cdot \mathrm{Br}(J/\psi \to \mu^+\mu^-) = 2.08 \pm 0.17(\mathrm{stat}) \pm 0.46(\mathrm{syst})$ nb. Using the muon impact parameter we have estimated the fraction of J/ψ mesons coming from B meson decays to be $f_b = 0.35 \pm 0.09(\mathrm{stat}) \pm 0.10(\mathrm{syst})$ and inferred the inclusive b production cross section. From the information on the event topology the fraction of nonisolated J/ψ events has been measured to be $f_{\mathrm{nonisol}} = 0.64 \pm 0.08(\mathrm{stat}) \pm 0.06(\mathrm{syst})$. We have also obtained the fraction of J/ψ events resulting from radiative decays of χ_c states, $f_\chi = 0.32 \pm 0.07(\mathrm{stat}) \pm 0.07(\mathrm{syst})$. We discuss the implications of our measurements for charmonium production processes.

PACS: 13.85.Ni; 14.65 Fy
Keywords: Beauty; Charmonium; QCD; Tevatron

1. Introduction

In high energy $p\bar{p}$ collisions the dominant contributions to J/ψ production are expected to come from the lowest order gluon-gluon fusion Feynman diagrams. The charmonium state is produced either directly [1], or through a $b\bar{b}$ pair followed by a decay $B \to J/\psi X$ [2,3]. Existing data from $p\bar{p}$ collider experiments UA1 [4] and CDF [5,6] indicate that gluon-gluon fusion processes alone fail to reproduce the observed J/ψ production rate. It has been argued [7] that, in addition to gluon-gluon fusion, the process of gluon or charm quark fragmentation, i.e. splitting of a virtual parton into a charmonium state and other partons, is an important source of J/ψ. Both fragmentation directly into J/ψ and fragmentation into χ_c followed by the radiative decay $\chi_c \to J/\psi + \gamma$ were included in the calculations of Ref. [7]. Fragmentation into χ_c was found to give the largest contribution. While this process is of higher order in the QCD coupling constant α_s, it is enhanced by a factor of ${p_T}^2/{m_c}^2$ (m_c is the charm quark mass) with respect to gluon-gluon fusion and thus may play a significant role at sufficiently high transverse momentum. Recently it was suggested that the production and subsequent decay of hybrid, metastable charmonium ($c\bar{c}g$) states might be yet another source of J/ψ [8].

Our measurement of the inclusive J/ψ production cross section presented in this paper is in agreement with the earlier results [4–6]. In addition, a detailed study of the J/ψ data, including the event topology, muon impact parameter, and the rate of χ_c radiative decays, allows us to estimate the role of various charmonium production mechanisms in $p\bar{p}$ collisions and to infer the inclusive b production cross section.

2. Detector and data selection

In this analysis we select opposite charge muon pairs in the mass range $M_{\mu\mu} < 6\,\mathrm{GeV}/c^2$. The analysis makes extensive use of all the main components of the DØ detector [9]: the muon spectrometer, the liquid-argon uranium calorimeter, and the central tracking detector. The muon spectrometer consists of three layers of proportional drift tubes and a magnetized iron toroid between the first two layers. The muon detector provides a measurement of muon momentum with a resolution of

$$\delta p/p = \left[\left(\frac{0.18(p-2)}{p}\right)^2 + (0.008p)^2\right]^{1/2}$$

(p in GeV/c).

The calorimeter provides confirmation of the muon track and information on the presence of other hard scattering products in the vicinity. The total thickness of the calorimeter plus the toroid varies from 13 to 15 interaction lengths and reduces the hadron punchthrough to a negligible level (<0.5%). The electromagnetic part of the calorimeter, with its fine segmentation and energy resolution for electrons and photons of $15\%/\sqrt{E(\mathrm{GeV})}$, has been used to detect the photon from the radiative decay of χ_c states. The central tracking system helps in identifying muons associated with the interaction vertex. The inner vertex chamber (VTX) has three cylindrical layers of cells of eight wires each. The spatial resolution in the $r-\phi$ plane is ≈ 60 μm. Muon track segments detected in the VTX chamber have been used in finding evidence for B particle decays as a source of muons.

The data sample comes from the 1992–1993 Tevatron collider run. Dimuon data are collected with a multilevel trigger. The hardware and software muon triggers are described elsewhere [10]. The inclusive J/ψ cross section determination and the inferred integrated b quark cross section are based on a data sample collected during the last half of the run, following major changes in the muon trigger electronics. The data correspond to a total integrated luminosity of 6.6 pb^{-1}. For this sample the events are required to have two muons at both hardware and software trigger levels. In the offline analysis two good quality muon tracks are required in the pseudorapidity range $|\eta_\mu| < 1.0$ ($\eta_\mu = -\ln[\tan(\theta/2)]$, where θ is the polar angle with respect to the beam axis). Both muon trajectories are required to be consistent with the reconstructed vertex position and to have a matching track in the central detector and at least 1 GeV energy deposition in the calorimeter. Each muon candidate is required to have at least one hit in the innermost layer of the muon detector. We exclude muon candidates in the re-

[1] Visitor from IHEP, Beijing, China.
[2] Visitor from Univ. San Francisco de Quito, Ecuador.

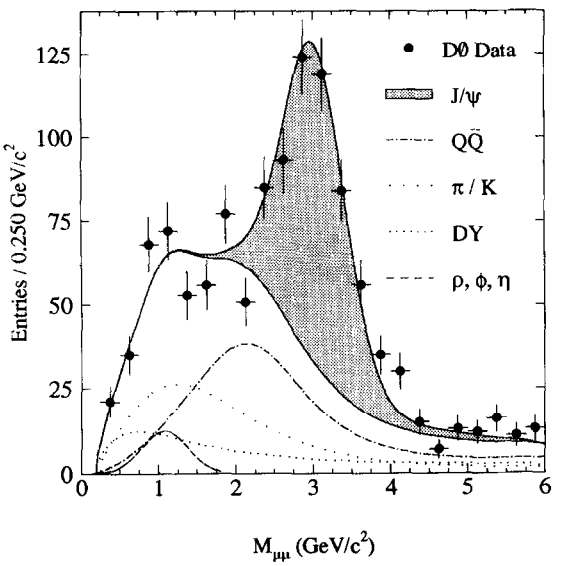

Fig. 1. The mass spectrum for opposite sign muon pairs. The fitted J/ψ signal and background contributions are shown separately.

gion $80° < \phi_\mu < 110°$, corresponding to the detector area near the Main Ring beam pipe where the muon chamber efficiency was low and poorly measured. We also restrict the pseudorapidity range for the dimuon to $|\eta| < 0.6$. In view of the modest dimuon mass resolution, $\approx 12\%$ at the J/ψ mass, we carry out a complete analysis of the dimuon data in the invariant mass range $M_{\mu\mu} < 6$ GeV/c^2. The total number of events used is 1146. The $M_{\mu\mu}$ distribution is shown as the solid points in Fig. 1. The fitted J/ψ signal and background contributions are discussed in the following sections.

To determine the relative rates of J/ψ production from B meson decays, f_b, and from radiative χ_c decays, f_χ, we use data from the entire run, with a total integrated luminosity of 13 pb^{-1}. The combination of the increased luminosity and looser trigger requirements results in a 60% increase in the number of J/ψ events available for the analysis.

3. Inclusive J/ψ production cross section

In addition to the J/ψ signal, the dominant contribution to the dimuon spectrum at $M_{\mu\mu} < 6$ GeV/c^2 is expected to come from processes involving heavy quarks, b and c. We distinguish the following classes of processes: (1) $B \rightarrow J/\psi X$; (2) direct charmonium production; (3) $b\bar{b}$ and $c\bar{c}$ events with both heavy quarks decaying semileptonically or with a sequential semileptonic decay $b \rightarrow c + \mu$, $c \rightarrow \mu$ (jointly denoted $Q\bar{Q}$); and the case where one muon comes from a b or c decay and the other from a decay of a π or K meson (4). Other mechanisms that yield opposite sign dimuons are (5) virtual photon decays, referred to as the Drell-Yan process [11], and (6) decays of light quark mesons such as ρ, ϕ and η.

Muons originating from b or c decays are accompanied by a collimated jet of hadrons that can be detected in the calorimeter. Gluon fragmentation into charmonium is also expected to produce muons embedded in jets. By contrast, muons from Drell-Yan events and those coming from direct charmonium production are expected to be isolated.

We use the dimuon mass, $M_{\mu\mu}$, the isolation of the more energetic muon, I_μ, and the dimuon momentum transverse to the jet axis, $p_{T\,\mathrm{rel}}^{\mu\mu}$, to distinguish between various sources of dimuon events. We measure the isolation parameter for a muon, I_μ, by summing the energy in the calorimeter cells traversed by the muon and their two nearest neighbors (i.e. in a tower of size $\Delta\eta \times \Delta\phi = 0.5 \times 0.5$) and subtracting the expected energy deposition for a minimum ionizing particle with the given momentum. If the other muon of the pair lies within an $\eta - \phi$ cone of radius $\Delta R = 0.6$ about the direction of the first muon, the energy loss of that muon is subtracted as well. If there is a jet in the event with a transverse energy greater than 8 GeV within a cone of radius $\Delta R = 0.7$ about the direction of the dimuon momentum, it is used to calculate $p_{T\,\mathrm{rel}}^{\mu\mu}$, otherwise $p_{T\,\mathrm{rel}}^{\mu\mu}$ is set to zero.

For each of the six dimuon production processes mentioned above, we generate a sample of Monte Carlo events. The process $B \rightarrow J/\psi X$ serves as a paradigm for the 'nonisolated' J/ψ production, including the possible gluon fragmentation process, for which no simulation program is currently available. Similarly, direct charmonium production is used as a template for all possible sources of isolated J/ψ. To simulate direct charmonium production we use the explicit formulae for gluonic production of P wave $c\bar{c}$ states given by Humpert [12]. We use the ISAJET [13] Monte Carlo generator which employs the EHLQ parton distribution functions [14].

Each ISAJET Monte Carlo sample is passed through a program simulating the effects of the detector [15] and trigger responses and then processed with the stan-

dard offline reconstruction program. For all six processes we have formed normalized probability distributions in the three selected physics variables, $M_{\mu\mu}$, $p_{T\,\mathrm{rel}}^{\mu\mu}$, and I_μ. The distributions are combined to form a normalized likelihood function which is maximized with respect to coefficients that correspond to the contribution of each process.

The fitted contributions to the dimuon spectrum from various processes are shown in Fig. 1. The total estimated number of J/ψ events is $407 \pm 28(\mathrm{stat}) \pm 55(\mathrm{syst})$. The fraction of J/ψ events attributed to nonisolated production is determined to be $f_{\mathrm{nonisol}} = 0.64 \pm 0.08(\mathrm{stat}) \pm 0.06(\mathrm{syst})$. The systematic uncertainty in the number of J/ψ events and f_{nonisol} is estimated by testing the stability of the fits with respect to changes in the fit assumptions. This includes varying the number of subprocesses considered in the fit, changing the shapes of the mass and isolation distributions, and fitting using only the mass and isolation distributions. The I_μ distribution for events in the mass range from 2 to 4.4 GeV/c^2, together with the four largest contributions, is shown in Fig. 2. Fig. 3 shows the distribution of the dimuon transverse momentum $p_T^{\mu\mu}$ for the same mass range. We emphasize that the $p_T^{\mu\mu}$ distributions are not used in the fit, and therefore the observed agreement between the data and the sum of all QCD subprocesses considered in the analysis provides support for this approach. In Figs. 1–3, we also show individual contributions from different processes included in the fit. However, the limited statistics of the data and the nonresonant character of most of those processes prevent us from making a reliable measurement of the cross section for each individual process. More details on the fitting procedure can be found in Ref. [16].

As a result of the fit, each event is assigned a relative probability of originating from a given process. To obtain the inclusive J/ψ transverse momentum spectrum, we weight the experimental $p_T^{\mu\mu}$ distribution with the probabilities for nonisolated and isolated J/ψ. To correct for the momentum smearing of the muon, we have separately unfolded the resulting J/ψ transverse momentum spectra using the technique of Ref. [17] and added the two unsmeared distributions together. The total unfolded spectrum, corrected for the acceptance and efficiency determined with simulated events, is used to calculate the differential J/ψ cross section $d\sigma/dp_T$.

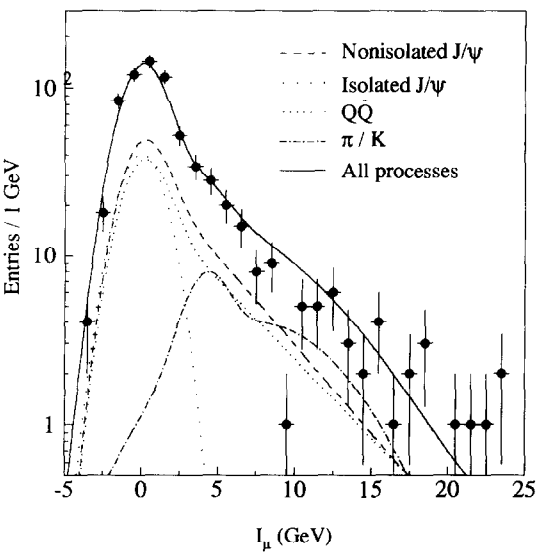

Fig. 2. The isolation distribution for opposite sign muon pairs in the mass range $2 < M_{\mu\mu} < 4.4$ GeV/c^2. The solid line is the fitted sum of the J/ψ signal and background contributions. Also shown are the contributions from nonisolated and isolated J/ψ production, as well as $Q\bar{Q}$, and π/K decays.

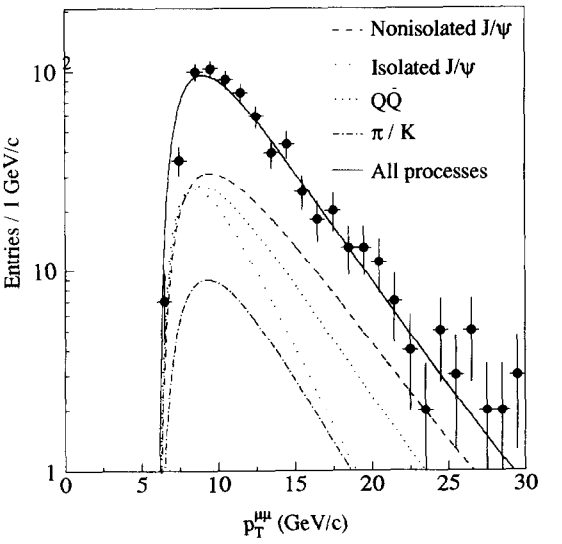

Fig. 3. The transverse momentum distribution for opposite sign muon pairs in the mass range $2 < M_{\mu\mu} < 4.4$ GeV/c^2. The solid line is the fitted sum of the J/ψ signal and background contributions. Also shown are the contributions from nonisolated and isolated J/ψ production, $Q\bar{Q}$, and π/K decays.

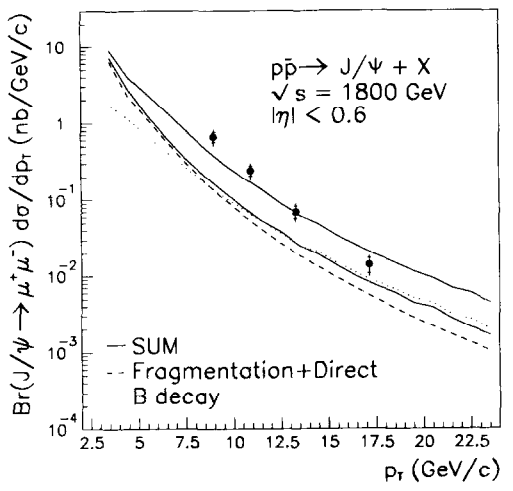

Fig. 4. The product $d\sigma/dp_T \cdot \mathrm{Br}$ vs p_T for $J/\psi \rightarrow \mu^+\mu^-$. The dotted line corresponds to J/ψ production through B meson decays. The dashed line corresponds to prompt J/ψ production. The sum, with theoretical uncertainties [3], is delimited by the two solid lines.

The combined acceptance and efficiency as a function of p_T increases from 1% at 8 GeV/c to a plateau of 10% at 15 GeV/c. The total systematic uncertainty is estimated to be 22%. It includes contributions from trigger efficiency (15%), background subtraction (14%), offline dimuon selection cuts (6%), and the integrated luminosity (5.4%).

Finally, the acceptance of the two muons depends on the unknown polarization of the parent J/ψ meson. Our results are presented for the case of zero polarization. For the extreme cases of 100% longitudinal and transverse polarization, the estimated cross section is changed by +20% and −25%, respectively.

For the integrated cross section we obtain

$$\sigma(p\bar{p} \rightarrow J/\psi + X) \cdot \mathrm{Br}(J/\psi \rightarrow \mu^+\mu^-)$$
$$= 2.08 \pm 0.17(\mathrm{stat}) \pm 0.46(\mathrm{syst})\ \mathrm{nb},$$
$$p_T > 8.0\ \mathrm{GeV}/c, \quad |\eta| < 0.6.$$

The inclusive J/ψ production cross section as a function of transverse momentum is shown in Fig. 4. The data points are shown with the statistical uncertainties and with the total of statistical and systematic uncertainties added in quadrature. The spectrum agrees closely in size and shape with the J/ψ inclusive cross section measured by the CDF Collaboration [5,6]. Also plotted in Fig. 4 are theoretical predictions for the J/ψ production cross section. They agree with our measurement within the total experimental and theoretical uncertainty but are somewhat less steeply falling with p_T.

4. J/ψ production from B meson decays

To determine the fraction f_b of J/ψ events originating from B meson decays, we examine the distribution of the impact parameter of the muons relative to the event vertex in the transverse plane.

The beam position in the $r - \phi$ plane is determined collectively for all events occurring during a running period lasting a few hours. Tracks from the central drift chamber (CDC) are used to determine the z coordinate (along the beam) of the primary vertex. CDC tracks consistent with originating from the primary vertex are extrapolated to the VTX chamber. VTX track parameters and the z coordinate of the event vertex are stored for each event and used at the end of the run to fit the parameters of the beam trajectory: x_0, y_0 and slopes dx/dz and dy/dz.

To calculate the muon impact parameter, each muon is required to have a matching track in the CDC and in the VTX chamber. The track matching efficiency is $\approx$ 50%. The impact parameter is defined as the distance of closest approach between the track and the primary vertex in the transverse plane. The sign is defined as positive (negative) if the track crossed the associated jet axis in front of (behind) the primary vertex. If there is no associated jet, the dimuon direction is used as the reference axis. We have performed a simultaneous mass and impact parameter maximum likelihood fit [16] to the opposite sign dimuon data in the mass range 2 to 4.4 GeV/c^2 and the impact parameter range −0.08 cm to 0.16 cm. The fit includes four processes: (1) $B \rightarrow J/\psi$, (2) direct charmonium production, (3) $Q\bar{Q}$, and (4) Drell-Yan production. The VTX track matching requirement suppresses the events with π and K decays. Fig. 5 shows the muon impact parameter distribution together with the fitted contributions from processes (1)–(3).

The total number of fitted J/ψ events is 143 ± 17, over a background of 120 ± 15 $Q\bar{Q}$ and 8 ± 4 Drell-Yan events. The fitted value of the fraction of J/ψ mesons coming from B meson decays is f_b = 0.35 ± 0.09(stat)±0.10(syst). For this sample the

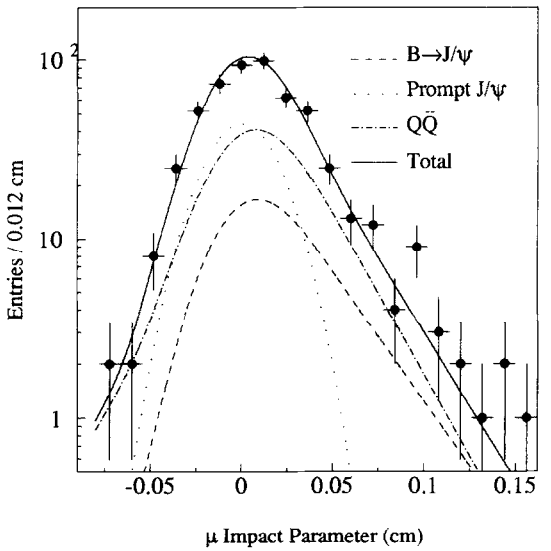

Fig. 5. Distribution of the impact parameter with respect to the event vertex in the transverse plane for muons in the J/ψ region. Also shown are the fitted contributions from prompt J/ψ (dotted line), B produced J/ψ (dashed line), and the $Q\bar{Q}$ continuum (dashed-dotted line).

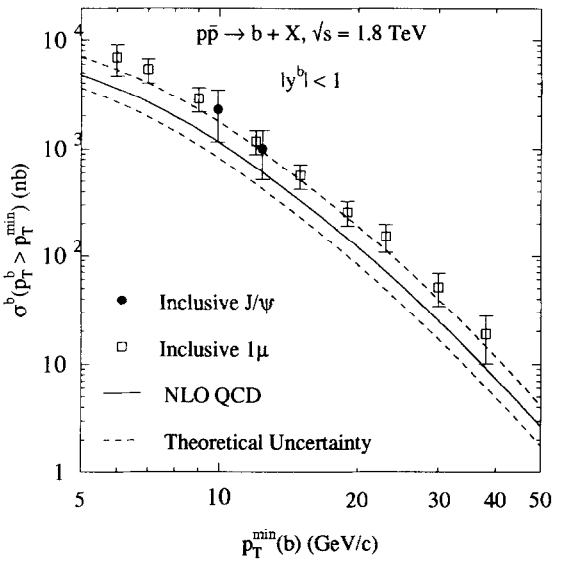

Fig. 6. Integrated b quark production cross section vs $p_T^{\min}(b)$. The full circles correspond to DØ J/ψ data (this work) and the open squares correspond to DØ single muon data [20]. The curve represents the QCD NLO prediction [21]. This prediction uses $m_b = 4.75$ GeV/c^2 and the MRSD0 structure functions with $\Lambda^5_{\overline{\rm MS}} = 140$ MeV. The theoretical uncertainty results from choosing $100 < \Lambda^5_{\overline{\rm MS}} < 187$ MeV, and the factorization and the renormalization scale μ in the range $\mu_0/2 < \mu < 2\mu_0$, where $\mu_0 = \sqrt{m_b^2 + \langle p_T^b \rangle^2}$.

mean value of the J/ψ transverse momentum is 11.8 GeV/c. The CDF Collaboration has determined f_b as a function of the J/ψ transverse momentum by measuring the decay distance of the dimuon in the transverse plane [6,18]. The two experiments are in good agreement in the overlap region, $p_T > 8$ GeV/c.

To determine the b quark cross section (the average of the b and $\bar{b}$ quark inclusive cross sections) we employ a technique first used by the UA1 Collaboration [19]. We scale the measured J/ψ inclusive production cross section by the following factors:

(1) the predicted Monte Carlo acceptance for b quarks with transverse momentum greater than $p_T^{\min}(b)$ that produce J/ψ's satisfying the kinematic cut $p_T > p_T^{\min}(J/\psi)$,

(2) the combined branching fractions $\mathrm{Br}(B \to J/\psi + X) \cdot \mathrm{Br}(J/\psi \to \mu^+\mu^-)$,

(3) the fraction f_b of J/ψ from B meson decays.

We define $p_T^{\min}(b)$ such that 90% of the b quarks remaining after application of the cut on the J/ψ transverse momentum $p_T > p_T^{\min}(J/\psi)$ have $p_T^b > p_T^{\min}(b)$. Fig. 6 shows the b quark integrated cross section for $p_T^{\min}(b) = 9.9$ and 12.4 GeV/c, corresponding to $p_T^{\min}(J/\psi) = 8$ and 10 GeV/c. The cross section is in excellent agreement with the DØ single muon results [20]. The lines show next to leading order (NLO) QCD predictions [21] with theoretical uncertainties. Our results are consistent with the upper limit of the QCD band, corresponding to the choice $\Lambda^5_{\overline{\rm MS}} = 187$ MeV and the factorization and the renormalization scale $\mu = \mu_0/2$, where $\mu_0 = \sqrt{m_b^2 + \langle p_T^b \rangle^2}$.

5. *P* wave charmonium production

J/ψ production in the direct charmonium model proceeds predominantly via P wave states, χ_c, followed by their radiative decays, that is, $gg \to \chi_c \to J/\psi + \gamma$. The dominant contribution to J/ψ production through fragmentation is also expected to involve χ_c states. On the other hand, in B meson decays the fraction of J/ψ mesons coming from χ_c decays is $(23 \pm 8)\%$ [22].

We have obtained a χ_c signal [23] by performing a full reconstruction of the decay chain $\chi_c \to J/\psi + \gamma$, $J/\psi \to \mu\mu$. For events with a pair of opposite

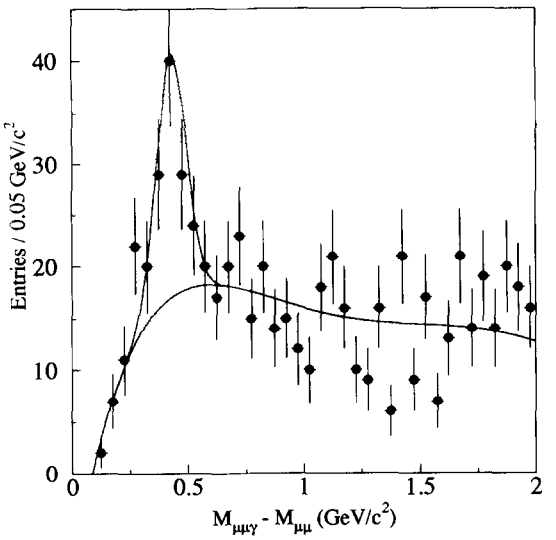

Fig. 7. Distribution in $\Delta M = M_{\mu\mu\gamma} - M_{\mu\mu}$ for dimuon events in the J/ψ region.

charge muons in the J/ψ mass region ($2 < M_{\mu\mu} < 4$ GeV/c^2) with $p_T^{\mu\mu} > 8$ GeV/c, we search for photons with energy greater than 1 GeV in the cone $\Delta R = 2$ about the dimuon direction. In the photon reconstruction, we employ a nearest neighbor clustering algorithm. Proceeding from a list of towers in the electromagnetic calorimeter, nearby towers are added to the cluster until there are no towers left with transverse energy E_T above 0.5 GeV. To ensure the maximum reconstruction efficiency for low energy photons and maximum discrimination against hadrons, a number of restrictions on the cluster shape is imposed. We define nth order moments $M^n(x)$ for a given variable x as

$$M^n(x) = \sum_{i=1}^{N} E_i x_i^n / M^0(x),$$

where N is the number of cells in the cluster, E_i is the energy deposited in the ith cell and x stands for η, ϕ or the coordinate along the shower development l. The following set of cuts is applied: $M^2(\phi) < 0.3$, $M^2(\eta) < 0.4$, $2 < M^1(l) < 13$, and $M^2(l) < 150$. Finally, the cluster is required to be separated from each muon by at least $\Delta R = 0.1$.

The difference between the invariant mass of the $\mu\mu\gamma$ and $\mu\mu$ systems, ΔM, is shown in Fig. 7. There is a clear χ_c signal near $\Delta M = 0.4$ GeV. The background comes from photons from the decay of particles belonging to the jet associated with the dimuon, as well as from random electromagnetic clusters from the underlying event. To estimate the background we have generated two distributions of ΔM by combining data from different dimuon events: (1) the jet associated with a dimuon is replaced with another jet from a different event, together with its associated photons; (2) a dimuon in one event is combined with any photon in any other event.

We fit the experimental distribution of ΔM with a combination of a Gaussian signal peak and the two background shapes. For the Gaussian we use the resolution of 0.063 GeV obtained from a Monte Carlo simulation. That gives us the best estimate of the size and shape of the background under the χ_c signal. The fit assigns 74 ± 13 events to the Gaussian. To make the signal estimate less dependent on the assumed Gaussian parameters, we subtract the fitted background from data in the ΔM interval 0.20–0.65 GeV. The result is $70 \pm 15(\text{stat}) \pm 12(\text{syst})$ χ_c events. The systematic uncertainty is estimated by varying the relative contribution of the two background shapes and by redoing the fit with the ΔM resolution changed by $\pm 30\%$ from its central value. In each case the result for the number of signal events varied by $\pm$ 8 events.

The combined correction factor for photon acceptance and reconstruction efficiency is obtained by the Monte Carlo method. With the efficiency of $30 \pm 4\%$, the measured fraction of J/ψ events coming from χ_c decay is $f_\chi = 0.32 \pm 0.07(\text{stat}) \pm 0.07(\text{syst})$. Using a similar technique, the CDF Collaboration obtained [24] $f_\chi = 0.45 \pm 0.05(\text{stat}) \pm 0.15(\text{syst})$ for $p_T > 6$ GeV/c.

Our result indicates that, contrary to the predictions of the direct charmonium production [1] and gluon fragmentation models [7], the prompt J/ψ production is not dominated by χ_c decay. Using our results on f_b and f_χ, and accounting for the contribution of 0.08 ± 0.03 from the decay chain $B \to \chi_c \to J/\psi$ [22], we obtain a fraction of $1 - f_b - f_\chi + 0.08 = 0.41 \pm 0.17$ of all J/ψ events that do not originate from either B or χ_c decay.

6. Summary and conclusions

We have measured the inclusive J/ψ production cross section as a function of J/ψ transverse momentum, p_T. For the kinematic range $p_T > 8$ GeV/c and

$|\eta| < 0.6$ we obtain $\sigma(p\bar{p} \to J/\psi + X) \cdot \mathrm{Br}(J/\psi \to \mu^+\mu^-) = 2.08 \pm 0.17(\mathrm{stat}) \pm 0.46(\mathrm{syst})$ nb. From the simultaneous fit to $M_{\mu\mu}$, $p_{T\,\mathrm{rel}}^{\mu\mu}$, and I_μ we determine the fraction of J/ψ events with a nonisolated dimuon, f_{nonisol}. Using the muon impact parameter we have estimated the fraction of J/ψ mesons coming from B meson decays, f_b. We have also obtained the fraction of J/ψ events resulting from radiative decays of χ_c states, f_χ.

The integrated b production cross section inferred from the J/ψ cross section and from the fraction of J/ψ events attributed to B decay is consistent with the upper edge of the NLO QCD band.

With $f_{\mathrm{nonisol}} = 0.64 \pm 0.11$ and $f_b = 0.35 \pm 0.14$, there is a fraction of $f_{\mathrm{nonisol}} - f_b = 0.29 \pm 0.17$ of all J/ψ events with nonisolated prompt dimuons. The large production of prompt, nonisolated J/ψ may be tentatively explained by gluon fragmentation [7]. Our measured inclusive J/ψ production cross section can be adequately described by theoretical predictions that include direct charmonium production, B decay, and gluon and c quark fragmentation processes.

However, in both the direct charmonium production [1] and gluon fragmentation models [7] the P wave charmonium states are predicted to play a prominent role, contrary to our results. We find that 0.41 ± 0.17 of all J/ψ events do not originate from either B or χ_c decay. The observation of a large component of J/ψ cross section which is neither due to B or χ_c decays warrants more study of possible sources of charmonium production in $p\bar{p}$ collisions at large transverse momentum.

Acknowledgements

We thank the Fermilab Accelerator, Computing, and Research Divisions, and the support staffs at the collaborating institutions for their contributions to the success of this work. We also acknowledge the support of the US Department of Energy, the US National Science Foundation, the Commissariat à L'Energie Atomique in France, the Ministry for Atomic Energy and the Ministry of Science and Technology Policy in Russia, CNPq in Brazil, the Departments of Atomic Energy and Science and Education in India, Colciencias in Colombia, CONACyT in Mexico, the Ministry of Education, Research Foundation and KOSEF in Korea, CONICET and UBACYT in Argentina, and the A.P. Sloan Foundation.

References

[1] R. Bayer and R. Ruckl, Z. Phys. C 19 (1983) 251.
[2] E.W.N. Glover, A.D. Martin and W.J. Stirling, Z. Phys. C 38 (1988) 473.
[3] M. Mangano, P. Nason and G. Ridolfi, Nucl. Phys. B 373 (1992) 295;
M. Mangano, private communication.
[4] UA1 Collaboration, C. Albajar et al., Phys. Lett. B 256 (1991) 112.
[5] CDF Collaboration, F. Abe et al., Phys. Rev. Lett. 69 (1992) 3704.
[6] CDF Collaboration, K. Byrum, Proceedings of the XXVII International Conference on High Energy Physics, Glasgow, Scotland, UK (20–27 July 1994), eds. P.J. Bussey and I.G. Knowles, Institute of Physics Publishing, Bristol and Philadelphia, p. 989.
[7] E. Braaten et al., Phys. Lett. B 333 (1994) 5483.
[8] F. Close, Phys. Lett. B 342 (1995) 369.
[9] DØ Collaboration, S. Abachi et al., Nucl. Instrum. Methods A 338 (1994) 185;
C. Brown et al., Nucl. Instrum. Methods A 279 (1989) 331.
[10] M. Abolins et al., Nucl. Instrum. Methods A 289 (1990) 543;
M.A.C. Cummings, D. Hedin and K. Johns, Proceedings of the Workshop on B Physics at Hadron Accelerators, Snowmass, CO (1993), p. 537;
M. Fortner et al., IEEE Transactions on Nuclear Science 38 (1991) 480.
[11] S.D. Drell and T.M. Yan, Phys. Rev. Lett. 25 (1970) 316.
[12] B. Humpert, Phys. Lett. B 184 (1987) 105.
[13] F. Paige and S. Protopopescu, BNL Report No. BNL38034 (1986), unpublished, release v6.49.
[14] E. Eichten et al., Rev. Mod. Phys. 56 (1984) 579.
[15] F. Carminati et al., CERN Program Library (December 1991), unpublished.
[16] C. Murphy, Inclusive J/ψ Production at DØ, Ph.D. thesis, Indiana University (1995), unpublished.
[17] G. D'Agostini, DESY Report No. DESY 94-099 (June 1994), unpublished.
[18] CDF Collaboration, F. Abe et al., Phys. Rev. Lett. 71 (1993) 3421.
[19] UA1 Collaboration, C. Albajar et al., Phys. Lett. B 256 (1991) 121.
[20] DØ Collaboration, S. Abachi et al., Phys. Rev. Lett. 74 (1995) 3548.
[21] P. Nason, S. Dawson and R.K. Ellis, Nucl. Phys. B 327 (1989) 49.
[22] M. Aguilar-Benitez et al., Phys. Rev. D 50 (1994) 1173.
[23] R. Demina, χ_c Production in $p\bar{p}$ Collisions at $\sqrt{s} = 1.8$ TeV, Ph.D. thesis, Northeastern University (1994), unpublished.
[24] CDF Collaboration, F. Abe et al., Phys. Rev. Lett. 71 (1993) 2537.